Available online at www.sciencedirect.com
ScienceDirect
Dyes and Pigments 74 (2007) 439–445
DYES and PIGMENTS
www.elsevier.com/locate/dyepig

Treatment of textile industry wastewater by supported photocatalysis

A. Alinsafi [a,b], F. Evenou [c], E.M. Abdulkarim [a], M.N. Pons [a,*], O. Zahraa [c], A. Benhammou [b], A. Yaacoubi [b], A. Nejmeddine [b]

[a] *Laboratoire des Sciences du Génie Chimique, UP 6811 CNRS-ENSIC-INPL, 1, rue Grandville, BP 20451, F-54001 Nancy Cedex, France*
[b] *Laboratoire d'Automatique et d'Etudes des Procédés, Université Cadi Ayyad, Faculté des Sciences Semlalia, Avenue Prince Mly Abdellah, BP 511, 40000 Marrakech, Morocco*
[c] *Département de Chimie-Physique des Réactions, UMR 7630 CNRS-ENSIC-INPL, 1, rue Grandville, BP 451, F-54001 Nancy Cedex, France*

Received 22 September 2005; received in revised form 11 December 2005; accepted 28 February 2006
Available online 24 April 2006

Abstract

Photocatalysis with TiO_2 particles immobilised either on a glass slide or on a non-woven glass fiber fabric has been applied to pure reactive dyes' (azoïc and metal phthalocyanines) solutions as well as textile wastewater containing the same dyes under UV and solar irradiation. Decolourization of textile wastewater was in the range 21–74% under solar irradiation, with COD removal rate between 0.2 and 0.9 g COD/h/m^2. These values are, however, strongly dependent upon the fine chemical structure of the dyes and the global composition of the wastewater. Performance prediction is therefore difficult but the results are encouraging for textile wastewater remediation. The increase of biodegradability is an additional positive factor, as it would improve the efficiency of a biological downstream treatment. No pH adjustment is necessary and wastewater at high pH can be treated directly after suspended solids removal.

Keywords: Titanium dioxide; Glass; Decolourization; Pollution abatement; Biodegradability

1. Introduction

Industrial wastewater is becoming more complex with the increasing diversity of manufactured products. It often contains bio-recalcitrant pollutants whose concentration and type vary to a great extent as a function of the consumer demands. This applies in particular to dyehouse wastewater. Dyes and especially the reactive ones are extensively used in textile industry. During the dyeing of fibers, such as cellulosic ones, substantial amounts of dyes are not fixed on the fabric: dyehouse wastewater usually contains about 10–50 mg/l of dyes in solution. Such concentrations are high enough to induce a remarkable colouring of the receiving water bodies where they are discharged.

Conventional biological methods have not proven to be particularly effective for coloured effluents. In most cases dyes are absorbed onto biomass without being really degraded [1]. Such pollution transfer is no more acceptable, as the sludge should be discarded in a sustainable manner.

Recently, there has been considerable interest in the utilization of advanced oxidation processes (AOPs) to destroy organic compounds. AOPs are based on the production of hydroxyl radicals as oxidizing agents to mineralize organic chemicals. Besides ozonation [2] and Fenton reaction [3], many efforts have been directed at the photodegradation of organic dyes by different UV irradiation systems, such as combinations with H_2O_2 [4–6], Fenton [3,5] or with a photocatalyst. The photocatalytic degradation of azoïc dyes in a TiO_2 suspension has been investigated by several research groups [7–10] all over the world. Hachem et al. [11] investigated the photocatalytic degradation of various dyes over TiO_2 deposited on glass slides and discussed its improvement by addition of hydrogen peroxide.

* Corresponding author. Tel.: +33 3 83 17 52 77; fax: +33 3 83 17 53 26.
E-mail address: Marie-Noelle.Pons@ensic.inpl-nancy.fr (M.N. Pons).

0143-7208/$ - see front matter © 2006 Elsevier Ltd. All rights reserved.
doi:10.1016/j.dyepig.2006.02.024

Although results have been reported using ZnO [12], the most used photocatalyst is certainly titanium dioxide (TiO_2) which presents good features of stability, non-toxicity and insolubility. However, its energy band gap is around 3.2 eV, which implies an excitation at wavelengths less than 400 nm that represent 5% of the solar spectrum. The advantage of using TiO_2 as photocatalyst lies in its capability to degrade toxic organic compounds [13], to reduce metallic ions [14], to improve the biodegradability of cellulosic effluents [15] and to decolourize a large variety of dyes in solution [16,17] or in solid mixtures [18]. Its basic efficiency can be enhanced by doping [19].

When TiO_2 suspensions are irradiated, electrons are excited from the valence band to the conduction one, generating positive holes and electrons:

$$TiO_2 + h\nu(< 400\ nm) \rightarrow TiO_2(e^- + h^+) \quad (1)$$

Electrons and holes can recombine (Eq. (2)) or react with other molecules, such as oxygen, generating reactive superoxide anions (Eq. (3)).

$$TiO_2(e^- + h^+) \rightarrow TiO_2 + \text{heat} \quad (2)$$

$$TiO_2(e^-) + O_2 \rightarrow TiO_2 + O_2^{\bullet -} \quad (3)$$

The positive holes can react with electron donors in the solution to produce hydroxyl radicals (Eqs. (4) and (5)) or directly oxidise organic matter (OM) at the semi-conductor surface (Eq. (6)).

$$TiO_2(h^+) + H_2O(ads) \rightarrow TiO_2 + H^+ + OH(ads)^{\bullet} \quad (4)$$

$$TiO_2(h^+) + OH^- \rightarrow TiO_2 + OH(ads)^{\bullet} \quad (5)$$

$$TiO_2(h^+) + \text{OM degradation intermediates} \rightarrow TiO_2 + OM^{\bullet +} \quad (6)$$

The hydroxyl radicals generated in the process are strong oxidants and react quickly with the organic matter adsorbed onto the catalyst (Eq. (7)), forming oxidised intermediates. If the treatment time is adequate, complete mineralization can be achieved.

$$OM + HO(ads)^{\bullet} \rightarrow \text{degradation intermediates} \rightarrow CO_2 + H_2O + \text{salts} \quad (7)$$

Simultaneously sulfur heteroatoms can be converted into sulfates and azo group nitrogen atoms into gaseous nitrogen [20].

When TiO_2 particles are used in suspension, they should be later removed from the effluent wastewater, but their small size (a few tens of nm) does not facilitate their recovery. TiO_2 can be immobilised on various supports such as carbon [21], glass [11,22], steel [23,24], cellulose fibers [25] and various adsorbents [26]. Our purpose has been to compare the photocatalytic efficiency of two glass-based supports (a rigid support made out of glass slides and a flexible one made of non-woven glass fiber fabric) for the degradation of individual reactive dyes (mostly azoïc dyes or phthalocyanines) or their mixture (real and synthetic textile wastewater) under solar and UV irradiation.

2. Materials and methods

2.1. Wastewater samples

Solutions of commercial reactive dyes (Drimarene (DR) from Clariant, Switzerland, and Procion from Dystar, Frankfurt, Germany) were prepared using de-ionised water at a concentration of 50 mg/l. Each dye is characterized by its wavelength corresponding to the maximum of UV–vis absorption. When possible, the CAS or ELINCS numbers are given: Yellow DR KR (CAS 75199-00-7) (C1) (azoïc) (λ_{max} = 437 nm), Orange DR KGL CDG (C2) (λ_{max} = 398 nm) (azoïc), Crimson Procion hexl (C3) (λ_{max} = 547 nm), Violet DR K2RL CDG (C4) (azoïc with Cu complex) (λ_{max} = 549 nm), Orange DR K3R CDG (CAS 83763-57-9) (C5) (λ_{max} = 488 nm) (azoïc), Red DR BT KBL CDG (C6) (λ_{max} = 515 nm), Yellow OR DR K2R CDG (CAS 68155-62-4) (C7) (λ_{max} = 390 nm) (azoïc), Green DR K5BL (CAS 71243-96-4) (C8) (λ_{max} = 658 nm) (Ni-phthalocyanine), Blue DR K2RL CDG (C9) (λ_{max} = 614 nm) (azoïc with Cu complex), Yellow DR K4G (C10) (ELINCS 412-530-3) (λ_{max} = 422 nm) (azoïc), Blue Procion herd (C11) (λ_{max} = 616 nm), Red DR K8B CDG (CAS 83400-12-8) (C12) (λ_{max} = 546 nm) (azoïc), Yellow Procion hexl (C13) (λ_{max} = 419 nm), Red DR K4BL CDG (C14) (λ_{max} = 542 nm) (azoïc), Blue DR KBL CDG (C15) (λ_{max} = 591 nm), Black DR (C16) (λ_{max} = 599 nm) (azoïc), Green DR K4GN (C17) (λ_{max} = 661 nm) (Ni-phthalocyanine). The range of initial pH of the 50 mg/l solution lies between 5.14 for C2 and 6.02 (for C8 and C12).

Different textile wastewater samples (WW1–WW12), collected in a cotton knit fabric dyehouse that uses the dyes previously listed, were tested. A synthetic textile wastewater (WW13) was prepared in the laboratory by mixing hydrolysed reactive dyes (Drimarene K2LR CDG Blue (2.78 mg/l); Drimarene KG Orange (3 mg/l); Drimarene K8B CDG Red (24.3 mg/l)), hydrolysed starch (2.78 mg/l), $(NH_4)_2SO_4$ (5.56 mg/l) and Na_2HPO_4 (5.56 mg/l) in de-ionised water. Hydrolysis was performed by heating the solutions at 80 °C for 1.5 h after adjustment at pH 12.

2.2. Photoreactor

The experimental set-up is based on a photocatalytic reactor of workable area 30 × 30 cm^2, made out of aluminium or stainless steel (Fig. 1). The wastewater to be treated is falling as a thin film from the top of the chamber onto titanium dioxide immobilised either on a non-woven fabric made of glass fibers

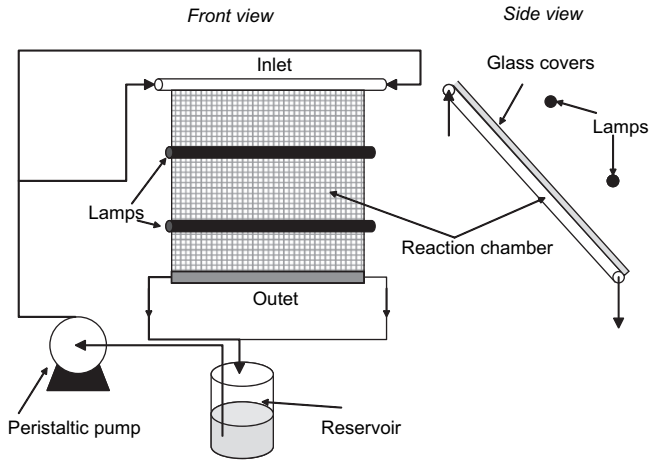

Fig. 1. Experimental set-up.

or on glass slides. The angle of slant was set at 37° to achieve a homogeneous distribution of the liquid. A transparent glass sheet covers the reacting chamber and permits to avoid the evaporation of the solution. The sample to be treated (250 ml of dye solution or 500 ml of textile wastewater) was stored in a reservoir and was continuously circulated in the system by a peristaltic pump at a constant flowrate of 2 ml/s that permits an optimal distribution of the liquid on the catalytic support. PTFE tubings were used. The reservoir was open to air to insure sufficient oxygenation. In case of solar irradiation, the average light flux during the experiment was measured by pyranometry (Pyranometer Skye, Campbell Scientific, Edmonton, Canada). Artificial irradiation was provided by two UV lamps (F15T8, BLB 15W, Duke, Essen, Germany) emitting around 365 nm, positioned parallel to the reactor. Light was turned on at the beginning of each experiment. The reactor was washed after every test by circulating de-ionised water with a few drops of hydrogen peroxide (30%) under UV or solar irradiation.

2.3. TiO_2 catalyst

Support A is a non-woven fabric made of glass fibers on which TiO_2 has been deposited and fixed by compression (Ahlstrom, Pont-Evêque, France) (Fig. 2a). According to the manufacturer the TiO_2 concentration on support A is about 20 g/m^2. Its specific area is 250 m^2/g. Two batches were used, denominated A1 and A2.

Support B is made of three glass slides (10 × 30 cm^2 each) on which TiO_2 particles (30 nm Degussa P25 particles made of 80% anatase and 20% rutile) have been deposited by a sol–gel method (Fig. 2b) [22]. The support was dip-coated in the solution, dried at 100 °C for 1 h and then calcinated at 450 °C. During heating, OH groups from the catalyst surface and the support can react and lose a molecule of water creating an oxygen bridge thus increasing the adherence of the catalyst to the support. Before deposition, the glass surface was treated with dilute HF solution and rinsed with NaOH in order to increase the number of OH groups. The suspension concentration

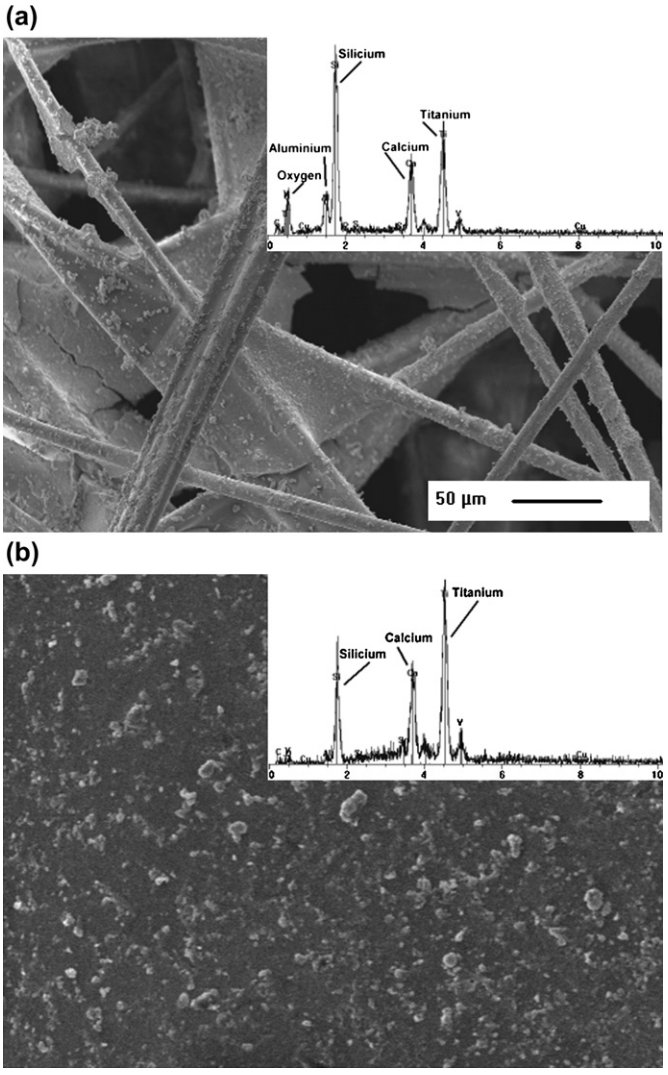

Fig. 2. Electron micrographs of TiO_2 deposited on fiber glass paper (support A) (a) and on glass (support B) (b), with the corresponding X-ray analysis spectra. On (b) TiO_2 particles are visible on fibers as well as the additive used to bind the glass fibers.

(4 g/l) was chosen so as to get thin deposits. This deposition process was carried out four times in succession in order to increase the total thickness. The slides had a final TiO_2 concentration of 2.8 g/m^2 with a specific area of about 50 m^2/g.

Analysis of both the supports by scanning electron microscopy (Jeol TSM 330 equipped with an X-ray probe) shows the presence of Ti, Si and Ca sites. Silicium and calcium originate from the glass (slide, fiber).

2.4. Analytical procedures

The reactions were monitored by UV–vis spectrophotometry using a SECOMAM (Domont, France) Anthelie Light device in the range 200–800 nm. Dissolved organic carbon (DOC) measurements were carried out on Apollo 9000 TOC analyser (Tekmar-Dohrmann, Mason, Ohio), after filtration (pore diameter 10 µm). Chemical oxygen demand (COD) was measured on a Hach 2400 (Loveland, Colorado, USA)

(Method 8000). Biological oxygen demand after 5 days was determined according to the standard Winkler method. pH and conductivity were measured using, respectively, a PHM 220 pH meter and a CDM 210 conductimeter (Radiometer Analytical SAS, Villeurbanne, France). With this method, the biodegradability is evaluated by the ratio $F = BOD_5/COD$.

To compare the efficiency of photocatalysis with respect to wastewater biodegradability, two methods are used: the first one is based on the calculation of the ratio BOD_5/COD after and before treatment, and the second one utilizes short-term respirometry batch tests [27]. Activated sludge (1.6 l) from a local domestic wastewater treatment plant was placed into a 2-l respirometer, equipped with an air-sparger and a mechanical stirrer. The dissolved oxygen concentration was monitored with an Orbisphere (Marin, Switzerland) probe connected to a PC for data logging. After measurement of the sludge endogeneous oxygen uptake rate and of oxygen mass transfer coefficient, the reference activity of the sludge is assessed by spiking the reactor with sodium acetate solution. The wastewater sample to be tested is then added. The short-term biological oxygen demand, BOD_{st}, was calculated as the volume of oxygen consumed for 20 min after the injection of the wastewater sample and was obtained by integration of exogenous oxygen uptake rate with respect to time. In this case, the biodegradability is evaluated by the ratio $F_{st} = BOD_{st}/COD$.

3. Results

3.1. Solar photocatalytic degradation of textile wastewater

Under solar irradiation on support A1 decolourization yields between 21% and 74% were achieved. Yield was calculated from the average of absorbance values measured at 436, 525 and 620 nm [2]. COD removal is in the range 23–55% depending upon the wastewater composition and it increases with exposure time (Table 1). The lowest efficiency was observed for WW5 with a high initial COD of 1.94 g/l. In terms of global COD removal rate, it varies between 0.2 g COD/h/m^2 of support for WW7 and 0.9 g COD/h/m^2 for WW3. These rates are somewhat lower than those indicated by Freudenhammer et al. [28] for biologically pre-treated textile wastewater. The decolourization yield for a pure solution of the yellow dye was of the same order of magnitude as for the industrial samples.

During treatment, temperature increased and pH changed slightly. It is difficult to clearly assess the effect of incident light flux on degradation. Highest COD abatement (55%) and a good decolourization are obtained for WW4 under the lowest average solar intensity. There could be two reasons for the absence of relationship in our case: the formation of water droplets during the experiment on the upper glass surface, even in case of relatively low temperature and the varying nature of the industrial wastewater samples. The complex mixture of dyes and other chemical substances is an important characteristic of real textile wastewater samples. Several studies report the negative impact of many additives (ionic species, organic solvents, humic substances, etc.) which are strong photodegradation inhibitors [29] as they compete with hydroxyl radicals and for the adsorption sites on the catalyst surface. These substances as well as the pH of textile wastewater influence or delay the photodegradation process. However, in spite of the wastewater variability, a decrease in the pollution in terms of COD and colour was observed under solar irradiation whatever be the sample. The alkaline pH favours the dye degradation, as noticed by Prieto et al. [7] and no pH adjustment is necessary.

Wastewater is considered to be difficult to treat biologically when $F = BOD_5/COD$ is lower than 0.3. Most of the samples under consideration present a poor initial biodegradability (Table 1), which increases significantly after treatment, except for two samples (WW3 and WW5).

3.2. UV photocatalytic degradation of textile wastewater

To compare the efficiency of the treatment under reproducible irradiation conditions, experiments were then conducted under artificial UV light.

The colour removal of the individual reactive dye solutions was first investigated for 1 or 2 h of irradiation, using both the TiO_2 supports and both the reactor materials. Table 2 summarizes the results. The decolourization yields obtained with

Table 1
Solar photocatalytic efficiency and biodegradability of wastewater samples before and after photocatalysis by solar irradiation

	Reaction time (h)	Initial pH	Initial COD (mg O_2/l)	F_0	Initial average absorbance[a]	%COD removal	%Decolourization	F_f	$F_b = F_f/F_0$	Final temperature (°C)	Average incident light flux (W/m^2)
WW 1A1_a	2	9.7	1166	0.22	0.38	30.6	25.6[a]	0.32	1.4	30.9	610.92
WW 2A1_a	2	9.6	1275	0.20	0.55	31	38.5[a]	0.32	1.56	27.5	620.38
WW 3A1_a	2	9.6	2083	0.17	0.69	32	51[a]	0.19	1.07	14.4	678.90
WW 4A1_a	3	8.5	1560	0.24	0.31	55	58[a]	0.41	1.70	33.1	204.25
WW 5A1_a	3	7.4	1940	0.21	0.29	23	21[a]	0.20	0.97	22.2	351.04
WW 6A1_a	5	7.2	1000	0.28	0.29	50	74[a]	0.48	1.71	26	n.d.
WW 7A1_a	5	8.5	800	0.35	0.19	50	48[a]	0.45	1.29	29.2	n.d.
Yellow dye (C7)B_i	2	5.22	n.d.		0.3		42 (at 390 nm)				n.d.

A1: support A1, B: support B, _i: stainless steel reactor, _a: aluminium reactor; n.d. = not determined.
[a] Average absorbance value at wavelengths 436, 525 and 620 nm.

Table 2
Decolourization and mineralization yields of investigated dyes under UV irradiation

Dye solution	Reaction time (h)	Initial pH	Final pH	%DOC removal	%Decolourization	%COD removal
C1A1_a	1	5.63	7.12	79.7	100	
C2A1_a	1	5.14	6.7	73.5	100	
C3A1_a	1	6	6.97	84.1	99.2	
C4A1_a	1	5.37	6.85	62.5	99.9	
C5A1_a	1	5.45	7.01	49.6	99.1	
C6A1_a	1	5.77	6.85	55.4	96.6	
C7A1_a	1	5.22	6.74	54.1	99.7	
C8A1_a	1	6.02	6.68	56.7	99.7	
C9A1_a	1	5.9	6.81	67	87.0	
C10A1_a	1	5.66	6.8	65.1	100	
C11A1_a	1	5.92	6.86	59.3	70.5	
C12A1_a	1	6.02	7.01	69.4	89.3	
C13A1_a	1	5.63	7.19	78	88.8	
C14A1_a	1	5.64	6.86	69.4	97.8	
C15A1_a	1	5.63	6.84	68.7	88.7	
C2B_a	2				63	95
C7B_a	2				89	49
C8B_a	2				25.3	76
C9B_a	2				44.5	38.2
C13B_a	2	5.6	7.21		35.7	
C16B_a	2				94	60
C17B_a	2				40	58.8
C8A2_a	1				60	
C9A2_a	1				46.4	
C13A2_a	1	4.9	6.2		75.7	
C9A2_i	2	6.2			33.8	
C16B_i	2	5.2			67	

support A in the aluminium reactor for an irradiation time of 1 h are all very high. Obviously, decolourization is easier than organic matter removal, although it depends upon the dye chemical structure. Ni-phthalocyanines (C8 and C17) as well as azoic dyes are degraded, probably by the destruction of the phthalocyanine ring [30]. A slight increase in pH and temperature was observed during the treatment. In spite of the increase in irradiation time, the decolourization yields obtained with support B were much lower than with support A1. Theoretically, the number of active sites on support A should be roughly proportional to the specific area (250 m^2/g) and the load (20 g/m^2), both of which are much higher than for support B (50 m^2/g and 2.8 g/m^2, respectively). However, the ratio of the decolourization yields is not in the order of magnitude of the theoretical ratio of active sites (i.e. 36). Not all the sites of support A are probably active. It could be also observed that the quality of support A varies depending upon the manufactured batch: the results obtained for dyes C8, C9 and C13 with support A2 were not as good as with support A1.

The reactor material has an effect on the treatment efficiency. Experiments were run on one hand with dye C9 and support A1 and on the other with dye C16 and support B. In both the cases better yields were obtained with the aluminium reactor. There is a probable reaction of aluminium with the liquid solution, with a partial dissolution of the metal and precipitation on the support. This can be visualized by the appearance of deposits on support A after use (Fig. 3). These deposits represent compounds generated by the incomplete mineralization of the organic pollution adsorbed initially onto the catalyst. They can reduce the activity of the TiO_2 catalyst by competition for the adsorption sites with hydroxyl radicals, and therefore decreases the treatment efficiency [31]. Aluminium could be detected by X-ray analysis. It cannot be excluded that a fraction of the dye is adsorbed on the reactor aluminium surface but aluminium may also enhance the photocatalytic activity of TiO_2 [32] especially at the slightly acidic pH of the pure dye solutions. Sulfates produced as sulfur can be found in some deposits.

The effect of hydrolysis and initial pH was investigated with three dyes (C8, C9 and C16) with the stainless steel reactor. The results are shown in Fig. 4.

In real textile wastewater, dyes are hydrolysed during the dyeing stage. Hydrolysis occurs between the chemical component RX and water with the exchange of X (for example a carbon chain) and OH groups: $RX + HOH \rightarrow ROH + HX$. No effect was observed for the black dye C16, while the decolourization was improved for the blue dye C9, showing here also the importance of the chemical structure.

As the isoelectric pH of TiO_2 is equal to 6.3, a pH effect was expected. It was not observed and it could be due to the interference of the glass silica, whose isoelectric pH is around 2 and that is present in much higher proportion in both the

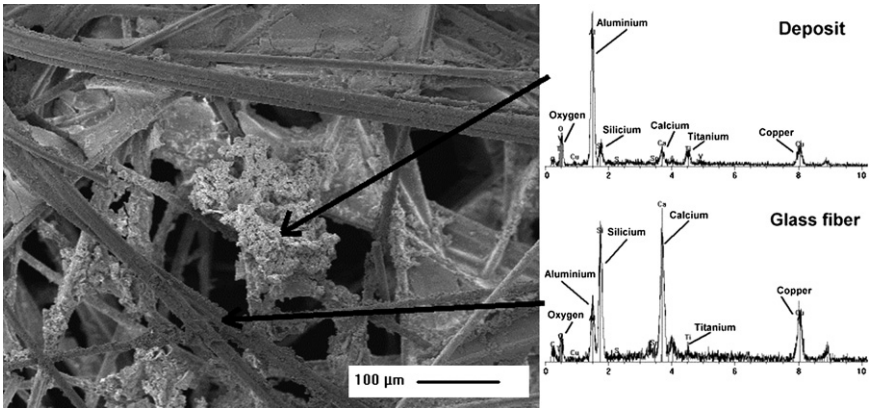

Fig. 3. Electron micrographs of support A after use in the aluminium reactor with the X-ray analysis spectra of a deposit and of a glass fiber.

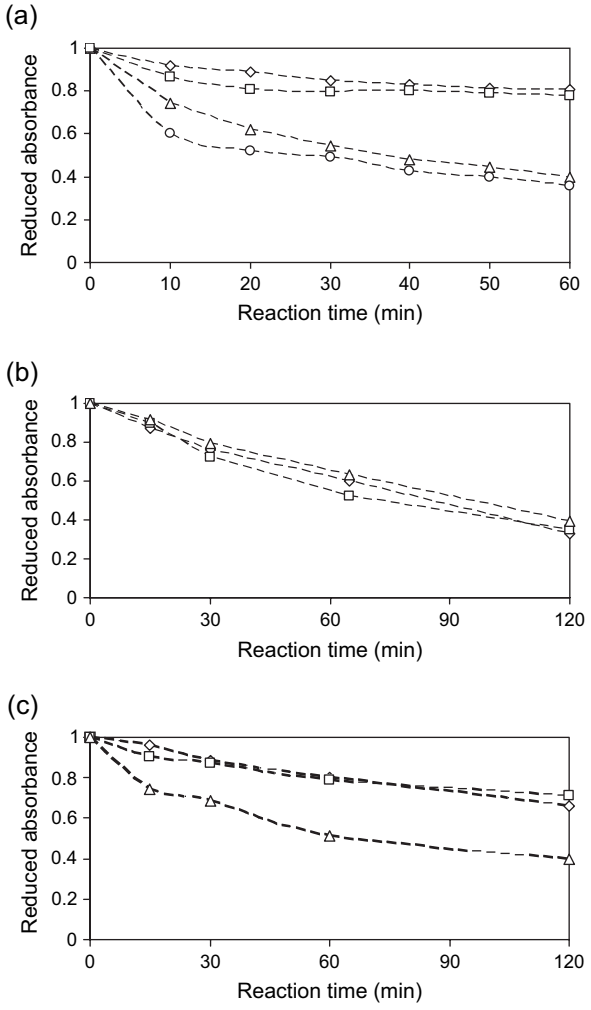

Fig. 4. Effect of pH and hydrolysis on decolourization kinetics of some reactive dyes (a) C8 (at 658) (◇) pH 6.0 on support B, (Δ) pH 6 on support A, (○) pH 10 on support A, (□) pH 10 on support B; (b) C16 (at 599 nm) on support A, (◇) pH 5.2, non-hydrolysed, (□) pH 10, non-hydrolysed, (Δ) after hydrolysis; (c) C9 (at 614 nm) on support A, (◇) pH 6.2, non-hydrolysed, (□) pH 10, non-hydrolysed, (Δ) after hydrolysis.

supports than TiO_2. Silica bound to TiO_2 has been recently recognized to enhance the degradation of some aqueous pollutants [33].

The degradation of real textile wastewater under UV irradiation was then investigated (Table 3). Better decolourization was achieved with support A than for support B for WW11 and WW12, but the inverse trend was observed for WW13, which is a synthetic textile wastewater with a low COD concentration. As with solar irradiation pH decreases during the reaction. The order of magnitude of the yields, both in terms of decolourization and organic matter removal, is similar for support A under solar and UV irradiation, even with a reaction time of 5 h. They are much lower than those observed under UV irradiation for the dye solutions and the support A1. Sunlight does not contain a large proportion of UV radiation (about 5%) and better yields could have been expected with full UV irradiation. Other phenomena, such as photosensitizing oxidation and reduction, can occur with sunlight [34], which might compensate for the lower abundance of UV radiation. No drastic effect of the reactor material was noticed: at least it cannot be differentiated from an effect due to the chemical composition of the sample.

Biodegradability after treatment was assessed by short-term respirometry. The biodegradability change is quantified by the ratio of $F_{stb} = F_{stf}/F_{st0}$: it increases significantly for three of the five tested cases (WW11 with support A, WW12 with supports A and B) and decreases for WW11 with support B. Due to the low COD load of WW13, it is possible that limited accuracy can be expected in this case and no conclusion can be drawn for its biodegradability.

At the end of the series of photocatalysis tests with the stainless steel reactor, microphotographs of support A were taken. Some deposits could be seen on the glass fibers after the use of the aluminium reactor. Their chemical nature could not be elucidated by X-ray analysis.

4. Conclusion

Supported photocatalysis has been applied to pure reactive dyes' solutions as well as real textile wastewater. Pollution

Table 3
Efficiency of photocatalysis and biodegradability change under UV irradiation for wastewater samples

	Reaction time (h)	Initial pH	Initial COD (mg O_2/l)	F_{st0}	Initial average absorbance[a]	%COD removal	%Decolourization	F_{stf}	$F_{stb} = F_{stf}/F_{st0}$	Final pH
WW8A_i	5	11.10	363	n.d.	0.11	50.47	72.6[a]	n.d.	n.d.	n.d.
WW9A_i	5	10.44	2121	n.d.	0.33	n.d.	41.4[a]	n.d.	n.d.	n.d.
WW10A_i	5	10.20	590	n.d.	0.23	30.99	48[a]	n.d.	n.d.	n.d.
WW11A_a	5	11.9	461	0.029	0.20	41.6	45[a]	0.045	1.55	9.75
WW 11B_a	5	11.7	461	0.030	0.20	20	32[a]	0.024	0.80	10.7
WW 12A_a	5	11.56	440	0.012	0.25	44	78[a]	0.021	1.67	10.05
WW 12B_a	5	11.45	440	0.013	0.25	46.24	12.5[a]	0.020	1.54	10.10
WW 13A_a	5	7.72	70	n.d.	0.13	n.d.	41	n.d.	n.d.	9.22
WW 13A_a	7	7.72	70	n.d.	0.13	32	81	n.d.	n.d.	8.92
WW 13B_a	5	7.72	70	0.057	0.13	n.d.	73.3	0.063	1.10	7.42
WW 13B_a	7	7.72	70	n.d.	0.13	n.d.	74	n.d.	n.d.	8.69

A: support A, B: support B, _i: stainless steel reactor, _a: aluminium reactor; n.d. = not determined.
[a] Average absorbance value at wavelengths 436, 525 and 620 nm.

abatement as well as decolourization were observed with promising yields. They are, however, strongly dependent upon the chemical structure of the dyes and probably also of the other additives (salts, detergents, biocides…) present in the textile industry wastewater: performance prediction is therefore difficult. If colour removal was the basic goal of this work, the increase of biodegradability is an additional positive factor, as it would improve the efficiency of a biological downstream treatment. No pH adjustment is necessary and wastewater at high pH can be treated directly after suspended solids removal. Due to its structure the non-woven glass fiber fabric seems very promising for an environment-friendly pretreatment using solar irradiation. Further work includes tests for extended periods of time to investigate the ageing of the material, limit the deposition of photocatalysis residues, and improve construction of catalyst in order to have a good fixing of TiO_2 on glass silica.

Acknowledgements

The authors wish to thank TENMAR (Marrakech, Morroco) and Alstrohm. This work was partially supported by the Comité Franco-Marocain under project MA/02/49.

References

[1] Easton JR. The dye marker's view. In: Cooper P, editor. Colour in dyehouse effluent. Oxford: Society of Dyers and Colourists, The Alden Press; 1995. p. 9–21.
[2] Selcuk H. Decolorization and detoxification of textile wastewater by ozonation and coagulation processes. Dyes Pigments 2005;64(3):217–22.
[3] Kiwi J, Pulgarin C, Peringer P. Effect of Fenton and photo-Fenton reactions on the degradation and biodegradability of 2 and 4-nitrophenols in water treatment. Appl Catal B Environ 1994;3(4):335–50.
[4] Oussi D, Mokrini A, Esplugas S. Removal of aromatic compounds using UV/H_2O_2. Trends Photochem Photobiol 1997;1:77–83.
[5] Herrera F, Kiwi J, Lopez A, Nadtachenk V. Photochemical decoloration of Remazol Brilliant blue and Uniblue A in the presence of Fe(III) and H_2O_2. Environ Sci Technol 1999;33:3145–51.
[6] Georgiou D, Melidis P, Aivasidis A, Gimouhopoulos K. Degradation of azo-reactive dyes by ultra-violet radiation in the presence of hydrogen peroxide. Dyes Pigments 2002;52:69–78.
[7] Prieto O, Fermoso J, Nuñez Y, del Valle JL, Irusta R. Decolouration of textile dyes in wastewaters by photocatalysis with TiO_2. Sol Energy 2005;79:376–83.
[8] Chun H, Wang Y. Decolorization and biodegradability of photocatalytic treated azo dyes and wool textile wastewater. Chemosphere 1999;39(12):2107–15.
[9] Gonçalves MST, Pinto EMS, Nkeonye P, Oliveira-Campos AMF. Degradation of C.I. Reactive Orange 4 and its simulated dyebath wastewater by heterogeneous catalysis. Dyes Pigments 2005;64:135–9.
[10] Muraganandham M, Swaminathan M. Photocatalytic decolourisation and degradation of Reactive Orange 4 by TiO_2–UV process. Dyes Pigments 2006;68:133–42.
[11] Hachem C, Bocquillon F, Zahraa O, Bouchy M. Decolourisation of textile industry wastewater by the photocatalytic degradation process. Dyes Pigments 2001;49:117–25.
[12] Akyol A, Bayramoğlu M. Photocatalytic degradation of Remazol Red F3B using ZnO catalyst. J Hazard Mater 2005;124:241–6.
[13] Legrini O, Oliveros E, Braun AM. Photochemical processes for water treatment. Chem Rev 1993;93:671–98.
[14] Litter MI. Heterogeneous photocatalysis: transition metal ions in photocatalytic systems. Appl Catal B Environ 1999;23:89–114.
[15] Yeber MC, Rodriguez J, Freer J, Baeza J, Mansilla HD. Advanced oxidation of a pulp mill bleaching wastewater. Chemosphere 1999;39:1679–88.
[16] Zhang F, Zhao J, Shen T, Hidaka H, Pelizzetti E, Serpone N. TiO_2-assisted photodegradation of dye pollutants. II: adsorption and degradation kinetics of eosin in TiO_2 dispersions under visible light irradiation. Appl Catal B Environ 1998;15:147–56.
[17] Wang Y. Solar photocatalytic degradation of eight commercial dyes in TiO_2 suspension. Water Res 2000;34:990–4.
[18] Vautier M, Guillard C, Hermann JM. Photocatalytic degradation of dyes in water. Case study of indigo and of indigo carmine. J Catal 2001;201:46–59.
[19] Liu X, Chen X, Li J, Burda C. Photocatalytic degradation of azo dyes by nitrogen-doped TiO_2 nanocatalysts. Chemosphere 2005;61:11–8.
[20] Karkmaz M, Puzenat E, Guillard C, Herrmann JM. Photocatalytic degradation of the alimentary azo dye amaranth. Mineralization of the azo group to nitrogen. Appl Catal B Environ 2004;51:183–94.
[21] Fu P, Luan Y, Dai X. Preparation of activated carbon filers supported TiO_2 photocatalyst and evaluation of its photocatalytic reactivity. J Mol Catal A Chem 2004;221:81–8.
[22] Guillard C, Lachheb H, Houas A, Ksibi M, Elaloui E, Herrmann JM. Influence of chemical structure of dyes, of pH and inorganic salts on their photocatalytic degradation by TiO_2 comparison of the efficiency of powder and supported TiO_2. J Photochem Photobiol A Chem 2003;158:27–36.
[23] Chan AHC, Chan CK, Barford JP, Porter JF. Solar photocatalytic thin film cascade reactor for the treatment of benzoic acid containing wastewater. Water Res 2003;37(5):1125–35.
[24] Kuo WS, Ho PH. Solar photocatalytic decolorization of dyes in solution with TiO_2 film. Dyes Pigments 2006;71:157–62.
[25] Aguedach A, Brosillon S, Morvan J, Lhadi EK. Photocatalytic degradation of azo-dyes reactive black 5 and reactive yellow 145 in water over a newly deposited titanium oxide. Appl Catal B Environ 2005;57:55–62.
[26] Bhattacharyya A, Kawi S, Ray MB. Photocatalytic degradation of orange II by TiO_2 catalysts supported on adsorbents. Catal Today 2004;98:431–9.
[27] Brouwer H, Klapwijk A, Keesman KJ. Identification of activated sludge characteristics using respirometric batch-experiments. Water Res 1998;32(4):1240–54.
[28] Freudenhammer H, Bahnemann D, Bousseli L, Geissen SU, Ghrabi A, Saleh F, et al. Detoxification and recycling of wastewater by solar-catalytic treatment. Water Sci Technol 1997;35(4):149–56.
[29] Epling GA, Lin C. Photoassisted bleaching of dyes utilizing TiO_2 and visible light. Chemosphere 2002;46:561–70.
[30] Sun A, Zhang G, Xu Y. Photobleaching of metal phthalocyanine sulfonates under UV and visible light irradiation over TiO_2 semiconductor. Mater Lett 2005;59:4016–19.
[31] Hu C, Wang Y. Decolourisation and biodegradability of photocatalytic treated azo dyes and wool textile wastewater. Chemosphere 1999;39(12):2107–15.
[32] Franch MI, Peral J, Domènech X, Howe RF, Ayllón JA. Enhancement of photocatalytic activity of TiO_2 by adsorbed Al(III). Appl Catal B Environ 2005;55(2):105–13.
[33] Shariq Vohra M, Tanaka K. Photocatalytic degradation of aqueous pollutants using silica-modified TiO_2. Water Res 2003;37(16):3992–6.
[34] Epling GA, Lin C. Investigation of retardation effects on the titanium dioxide photodegradation system. Chemosphere 2002;46:937–44.